Critical role of CDK2 for melanoma growth linked to its melanocyte-specific transcriptional regulation by MITF

Jinyan Du,[1,2] Hans R. Widlund,[1,2] Martin A. Horstmann,[1,2,5] Sridhar Ramaswamy,[1,2,4] Ken Ross,[3] Wade E. Huber,[1,2] Emi K. Nishimura,[1,2] Todd R. Golub,[1,2,3] and David E. Fisher[1,2,*]

[1]Department of Pediatric Hematology/Oncology, Dana-Farber Cancer Institute and Boston Children's Hospital, Boston, Massachusetts 02115
[2]Melanoma Program in Medical Oncology, Dana-Farber Cancer Institute, Harvard Medical School, Boston, Massachusetts 02115
[3]Broad Institute, Massachusetts Institute of Technology, Cambridge, Massachusetts 02141
[4]Department of Medical Oncology, Massachusetts General Hospital, Harvard Medical School, Boston, Massachusetts 02129
[5]Present address: Universitäts Klinikum Eppendorf, Hamburg 20246, Germany
*Correspondence: david_fisher@dfci.harvard.edu

Summary

The genomic organization of the *CDK2* gene, which overlaps the melanocyte-specific gene *SILV/PMEL17*, poses an interesting regulatory challenge. We show that, despite its ubiquitous expression, CDK2 exhibits tissue-specific regulation by the essential melanocyte lineage transcription factor MITF. In addition, functional studies revealed this regulation to be critical for maintaining CDK2 kinase activity and growth of melanoma cells. Expression levels of MITF and CDK2 are tightly correlated in primary melanoma specimens and predict susceptibility to the CDK2 inhibitor roscovitine. CDK2 depletion suppressed growth and cell cycle progression in melanoma, but not other cancers, corroborating previous results. Collectively, these data indicate that CDK2 activity in melanoma is largely maintained at the transcriptional level by MITF, and unlike other malignancies, it may be a suitable drug target in melanoma.

Introduction

MITF is a *b*asic-*h*elix-*l*oop-*h*elix/leucine-*zip*per (bHLHZip) transcription factor whose mutation produces melanocyte defects in mouse (Silvers, 1979) and human (Tassabehji et al., 1994). MITF belongs to the MYC superfamily of transcription factors and binds the E box sequences CA(C/T)GTG (Hemesath et al., 1994; Hodgkinson et al., 1993; Tachibana et al., 1994). The three major pigmentation enzymes, TYR, TYRP1, and DCT, are thought to be transcriptional targets of MITF (Bentley et al., 1994; Hemesath et al., 1994; Yasumoto et al., 1994, 1995, 1997), suggesting that the pigmentation pathway in general is largely regulated by MITF's activity. An additional MITF target gene important for pigmentation is the *SILVER/PMEL17* gene (Du et al., 2003), which encodes the GP100/HMB45 antigen commonly utilized for melanoma diagnosis and immune therapy (Adema et al., 1993; Wagner et al., 1995). Mutation of *Silver/Pmel17* produces a significant pigmentation defect (resembling silver color) in mice (Silvers, 1979), further supporting MITF's role as a transcriptional regulator of pigmentation. However, MITF deficiency affects melanocyte viability rather than pigmentation per se, suggesting that transcriptional targets beyond pigment genes are likely important as well. While expression of many melanocytic markers is often lost in melanoma, MITF expression is usually (if not always) maintained in human melanoma specimens, suggesting that MITF might be particularly important for melanoma maintenance (reviewed in Chang and Folpe, 2001). One particular MITF target likely to be important for viability is BCL2 (McGill et al., 2002). However, BCL2 cannot fully mediate MITF's proliferation/survival effects, because MITF deficiency produces earlier melanocyte deficiency than *Bcl2* knockout. In addition, BCL2 overexpression cannot rescue clonogenic growth in the setting of MITF disruption in melanoma cells (McGill et al., 2002). Together, these observations suggest the existence of other target genes that are important for the proliferation/survival of melanocytes and melanomas.

One such candidate is *c*yclin-*d*ependent *k*inase 2 (CDK2). Until recently, CDK2 was thought to be a major cell cycle regulator, functioning during the G1/S transition and S phase (Ekholm and Reed, 2000). In vivo, CDK activity is largely regulated positively through association with the appropriate cyclins and negatively by CDK inhibitors. Genomic analysis reveals that the tran-

SIGNIFICANCE

Until recently, CDK2 was considered to be one of the essential cell cycle regulators during G1-S transition and S phase progression. However, *Cdk2* null mice develop almost normally, and blockage of CDK2 in colon carcinoma cells and several other cancer types had minimal effects on their proliferation, suggesting that CDK2 might not be a suitable target for cancer treatments. Our results suggest that CDK2 might be particularly important for melanoma proliferation. These observations also help to explain MITF's essential role in melanoma growth. The unique regulation of CDK2 expression in melanoma, correlating with drug sensitivity, may help predict patients' responses to CDK2-targeted cancer therapy.

scriptional start site of *SILVER* resides just 796 nucleotides away from the *CDK2* gene start site (head-to-head orientation) (Adachi and Lieber, 2002). The TATA-less CDK2 promoter has been studied in NIH3T3 mouse fibroblasts (Shiffman et al., 1996). Multiple transcription factor binding sites have been identified, and the sequence spanning −100 to +108 is sufficient for basal promoter activity in NIH3T3 cells, specifically attributed to two SP1 sites within this region (Shiffman et al., 1996). In addition, a serum-responsive *cis*-element is present in a 1.7 kb segment 700 bp upstream of the transcriptional start (Shiffman et al., 1996).

Importantly, CDK2's role as a key cell cycle regulator has been challenged recently. In colon cancer cell lines, cell cycle arrest caused by MAPK inhibition is mediated by CDK4, but not CDK2 inhibition (Tetsu and McCormick, 2003). Moreover, inhibition of CDK2 by CDKN1B/p27KIP1, a dominant-negative CDK2, RNAi, or antisense does not prevent these cells from proliferating (Tetsu and McCormick, 2003). In addition, engineered *Cdk2* null mice display no dramatic phenotype other than sterility of both genders, suggesting that CDK2 is essential for meiosis but not mitosis during normal development (Berthet et al., 2003; Ortega et al., 2003).

Since the nearby *SILVER* gene is expressed in a melanocyte-restricted fashion, we asked whether its transcriptional regulator, MITF, might also modulate *CDK2* expression specifically in melanocytes. We show that this is indeed the case, using quantitative RT-PCR measurements of CDK2 mRNA and Western analysis of CDK2 protein upon modulation of MITF levels, chromatin immunoprecipitations (ChIPs), and luciferase reporter assays. Moreover, CDK2 and MITF expression levels are tightly correlated in a panel of primary human melanomas and melanoma cell lines. Functional studies reveal that *CDK2* regulation by MITF is essential for melanoma clonogenic growth. In addition, CDK2 expression levels correlated closely with sensitivity to the CDK inhibitor roscovitine. Finally, we confirm recent evidence that CDK2 suppression is well tolerated in other malignancies, yet find that CDK2 is essential for melanoma clonogenic growth and that siRNA-mediated depletion of CDK2 suppresses cell-cycle progression and short-term as well as long-term proliferation of these cells.

Results

Human *CDK2-SILV* locus

Recently, we identified *SILV* as a transcriptional target of MITF (Du et al., 2003). BLAST searching (Altschul et al., 1997) mapped its transcriptional initiation site to 796 bp away from the transcriptional start of *CDK2* (head to head) (Adachi and Lieber, 2002) (Figure 1A). Of three E boxes matching the MITF consensus within this region, one was found to reside within a 111 bp region 90% identical between mouse and man, and this E box was found to be targeted by MITF for regulation of *SILV* expression in melanocytes (Du et al., 2003). Due to its proximity to the *CDK2* gene, we therefore asked whether this element, and MITF, might similarly regulate CDK2 expression in melanocytic cells (Figure 1A).

In vivo binding of MITF to the *CDK2*/*SILV* E2 region

To investigate in vivo occupancy by MITF of the *CDK2* upstream regulatory region, ChIP was carried out from multiple cell types. Shown in Figure 1B are representative results from 501mel (melanoma) and SW480 (colon cancer) cells, the latter lacking significant MITF expression. PCR primers spanned the E2 site as well as a negative control (E3 site) near the transcription initiation site of *CDK2*. This assay revealed that MITF is bound to the *CDK2* upstream regulatory region, but not the area spanning the first exon/intron boundary. No PCR products were observed in controls immunoprecipitated with either no antibody or control antibodies against BRN2 or CDK2. ChIP was also negative in SW480 cells (which lack MITF), providing a control for the specificity of the MITF antibody signal in melanoma cells. These results indicate that MITF directly binds the E2 element in melanoma cells, consistent with previous evidence that MITF binds to the same region in regulation of the *SILV* gene (Du et al., 2003) and suggesting a direct effect on *CDK2* transcription.

Transcriptional regulation of endogenous *CDK2* by MITF in the melanocyte lineage

To investigate whether MITF modulates endogenous *CDK2* gene expression in melanocytic cells, early passage primary human melanocytes and several melanoma cell lines (501mel, SKMEL5, SKMEL28, UACC62, and A375) were infected with adenoviruses expressing wild-type MITF, dominant-negative MITF, or vector control. Quantitative RT-PCR measurements revealed that wild-type MITF stimulated expression of CDK2 mRNA, while dominant-negative MITF repressed CDK2 transcripts in melanocytes (Figure 2A). Adenoviral infections revealed the same CDK2 regulation by MITF in all five melanoma cell lines tested (Figure 2A). Western blot analysis (Figures 2B and 2C) also revealed that wild-type MITF upregulated and dominant-negative MITF downregulated expression of endogenous CDK2 protein. In addition, in vitro kinase assays revealed that dominant-negative MITF dramatically repressed while wild-type MITF did not significantly augment endogenous CDK2 kinase activity (Figure 2B), suggesting that transcriptional regulation of CDK2 by MITF appears to be rate limiting for CDK2 kinase activity in these cells.

We also examined regulation of CDK2 expression via siRNA-mediated knockdown of MITF. This siRNA specifically depleted MITF but not CDK1, CDK6, or α-tubulin in melanoma cells (Figure 2D). Consistent with the results from overexpression of dominant-negative MITF, we observed significant reduction of CDK2 protein levels upon depletion of MITF (Figure 2D). In addition, this siRNA was able to downregulate two known MITF downstream targets, BCL2 and SILV (Figure 2D). To further demonstrate the specificity of this siRNA, we examined its effects in a colon carcinoma cell line (SW480) that does not express endogenous MITF and observed no changes in CDK2 or α-tubulin expression levels.

E box-dependent modulation of CDK2 reporters by MITF

To further assess the directness of this regulation, luciferase reporters containing the upstream *CDK2* region were transfected into 501mel human melanoma cells with or without cotransfected MITF. As shown in Figure 3A, the E2 site was critical for MITF responsiveness, while E1 appeared to be dispensable.

Mice heterozygous for dominant-negative *Mitf* alleles ($Mitf^{Mi\text{-}Or}$ and $Mitf^{Mi\text{-}mi}$) display ventral spotting (white belly spot) due to absence of melanocytes, whereas those heterozygous for null ($Mitf^{mi\text{-}ce}$ and $Mitf^{mi\text{-}VGA9}$) or hypomorphic ($Mitf^{mi\text{-}vit}$) alleles exhibit normal pigmentation, indicating that dominant-negative

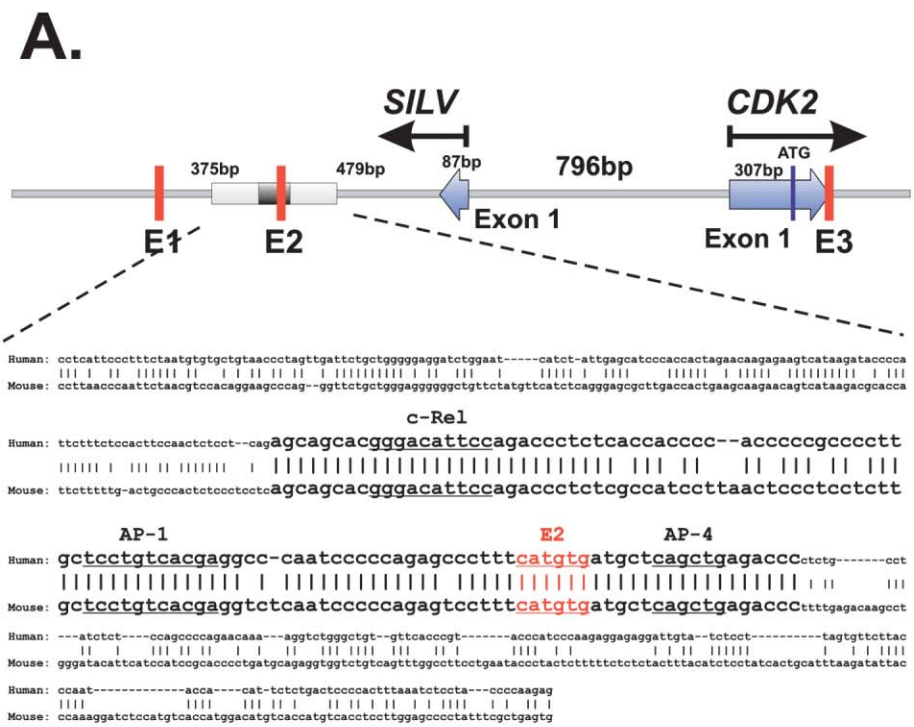

Figure 1. The human *CDK2-SILV* locus and binding of MITF to *CDK2 cis*-regulatory regions

A: The human *CDK2-SILV* locus and potential enhancer element. Exon ones are denoted by large arrows and reveal that the genes are encoded in a head-to-head configuration. Three E box consensus elements are highlighted in red and named E1–E3. The conserved DNA sequence surrounding the E2 site is shown in detail using a larger font. Predicted binding sites for additional transcription factors are underlined and annotated.

B: Binding of MITF to the endogenous, overlapping *CDK2* and *SILV cis*-regulatory region in melanoma cells versus colon carcinoma cells. Chromatin immunoprecipitations from 501mel or SW480 cells were performed as described in the Experimental Procedures. PCR products were resolved on 2% agarose by electrophoresis. DNA from lysates prior to immunoprecipitation was used as positive input control. The E2 primer set amplifies the E2-regulatory region, which is important for gene expression, while the E3 primer set amplifies a nearby region that is dispensable for gene expression (negative control), based upon reporter assays (see below and data not shown).

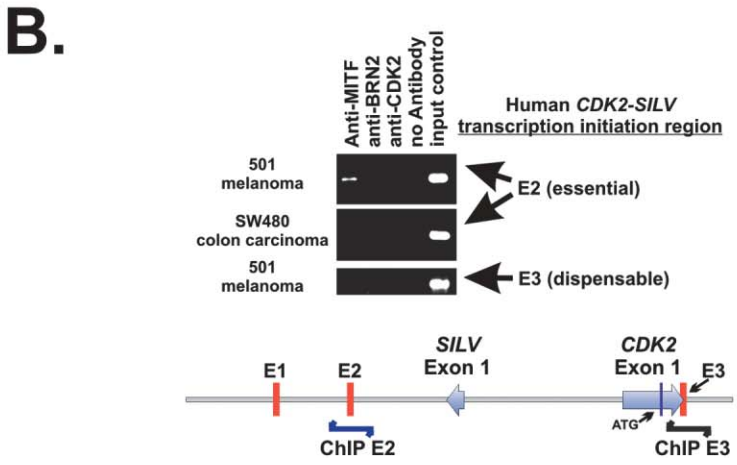

but not null mutants could interfere with the function of the wild-type allele. To assess whether the behavior of these mutant alleles would be reflected in transcriptional assays, CDK2 promoter luciferase reporters were cotransfected with mixtures of wild-type and mutant *Mitf* alleles (Figure 3B). These *Mitf* alleles have been used previously to demonstrate the transcriptional regulation of Cathepsin K by MITF in osteoclasts (Motyckova et al., 2001). The different versions of MITF were seen to be expressed at approximately comparable levels after transfection (Supplemental Figure S1 at http://www.cancercell.org/cgi/content/full/6/6/565/DC1/). Consistent with their dominant phenotype, $Mitf^{Mi\text{-}Or}$ and $Mitf^{Mi\text{-}mi}$ repressed cotransfected wild-type MITF activity on the CDK2 reporter by 80% and 90%, respectively. In contrast, the recessive mutant $Mitf^{mi\text{-}ce}$ did not interfere with the wild-type protein (Figure 3B).

To examine whether the E boxes are required for CDK2 transcription in the chromatin (integrated) context, the CDK2 upstream regulatory region was fused to the puromycin resistance gene and transfected into melanoma cells (Figure 3C). Here, using colony formation (reflecting integrated, chromatinized reporters), the E2 element was also found to be essential for transcriptional activity (Figure 3C). We also performed these colony formation assays in SW480, where there is no endogenous MITF expression, and found that a comparable number of colonies were formed with the wild-type and mutant constructs. These results suggest that the E2 element is not essential for

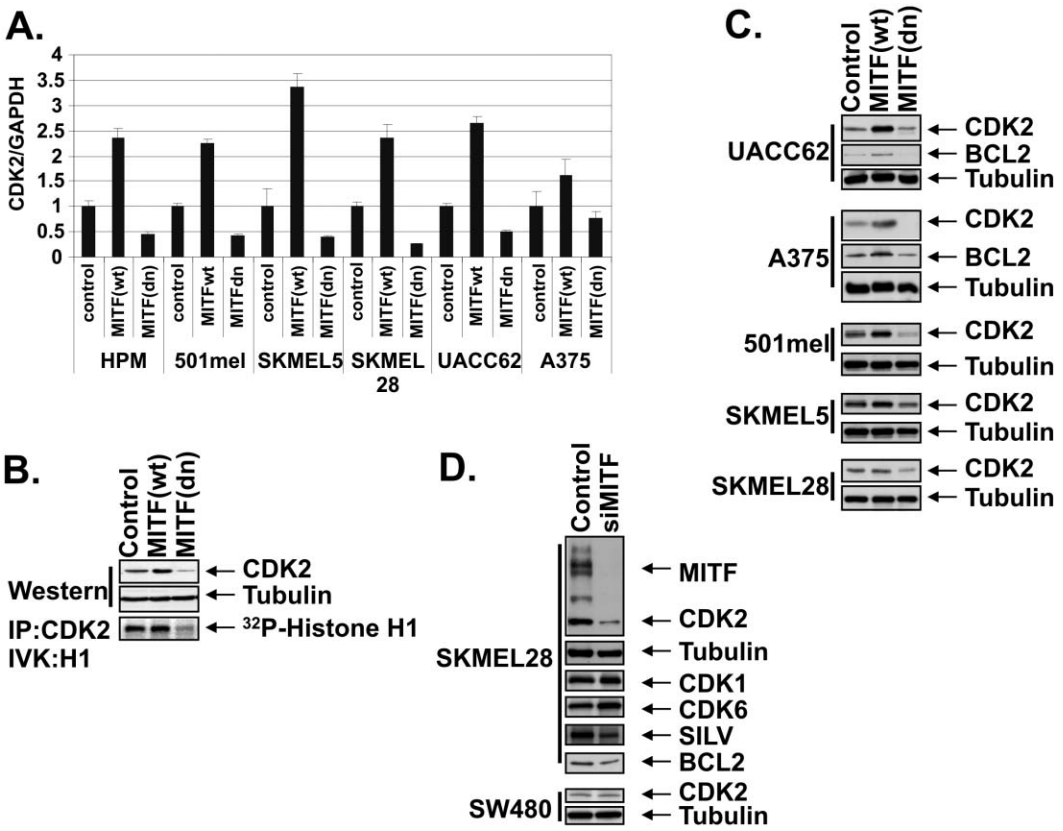

Figure 2. Transcriptional regulation of endogenous *CDK2* by MITF

A: Regulation of endogenous CDK2 mRNA levels by MITF in primary melanocytes (HPM) and melanoma cells. Total RNA was isolated 48–72 hr after infection. Quantitative RT-PCR was performed, and data were normalized to the expression level of the control gene. CDK2 mRNA level in the control adenovirus-infected sample was normalized to 1.

B: Regulation of CDK2 protein levels and kinase activities by MITF in primary melanocytes. CDK2 protein levels and kinase activities were assayed 72 hr after infection.

C: Regulation of CDK2 protein levels in five melanoma cell lines where CDK2 protein levels were assayed 48 to 72 hr after infection.

D: Downregulation of CDK2 expressions by siRNA-mediated depletion of MITF in melanoma cells (SKMEL28) but not in colon carcinoma cells (SW480). Melanoma cells are infected with retrovirus expressing control siRNA either against luciferase or against MITF. Puromycin was added to the culture media 48 hr after infection. Western analysis was performed 48 hr after selection.

CDK2 promoter activity in MITF-negative cells, which is consistent with the results presented in Figure 4.

Lack of transcriptional regulation of CDK2 by MITF in nonmelanocytes

We previously found that MITF could modulate SILV transcription in both nonmelanocytes and melanocytes (Du et al., 2003). We therefore asked whether CDK2 could be regulated by MITF in nonmelanocytes as well. CDK2 mRNA levels were examined in WI-38 fibroblasts after infection with adenovirus expressing a control protein or wild-type MITF. In contrast to the upregulation observed in the melanocyte lineage (Figure 2A), no significant difference in CDK2 mRNA levels was seen in these fibroblasts (Figure 4A). Consistent with previously published data (Du et al., 2003), we observed a significant upregulation of SILV mRNA upon wild-type MITF expression in these fibroblasts (Figure 4A). In addition, MITF had no effect on CDK2 reporter activity when cotransfected into 293, SW480, or T47D (Figure 4B and data not shown), nor was the E2 site important for basal expression (Figure 4C and data not shown). These data suggest a tissue-specific regulation of CDK2 expression by MITF in the melanocyte lineage.

Functional rescue by CDK2 after disruption of MITF in colony formation

To assess the functional importance of MITF's regulation of CDK2 expression, colony growth assays were performed using dominant-negative MITF (dn) (Widlund et al., 2002), which localizes to the nucleus (Figure 5A) and represses basal activity of an E box-driven reporter (Figure 5B). Sublethal doses of dominant-negative MITF suppressed melanoma colony formation by nearly 70% (Figure 5C). However, this suppression was rescued by overexpression of CDK2. In the reciprocal experiment (Figure 5D), dominant-negative CDK2 disrupted colony formation but was not rescued by wild-type MITF overexpression. These data suggest that disruption of MITF produces a block to cell growth due to depletion of CDK2, consistent with the model that CDK2 may be a functionally critical downstream effector of MITF for cell proliferation in melanoma cells. The data also suggest that suppression of CDK2 is measurably dele-

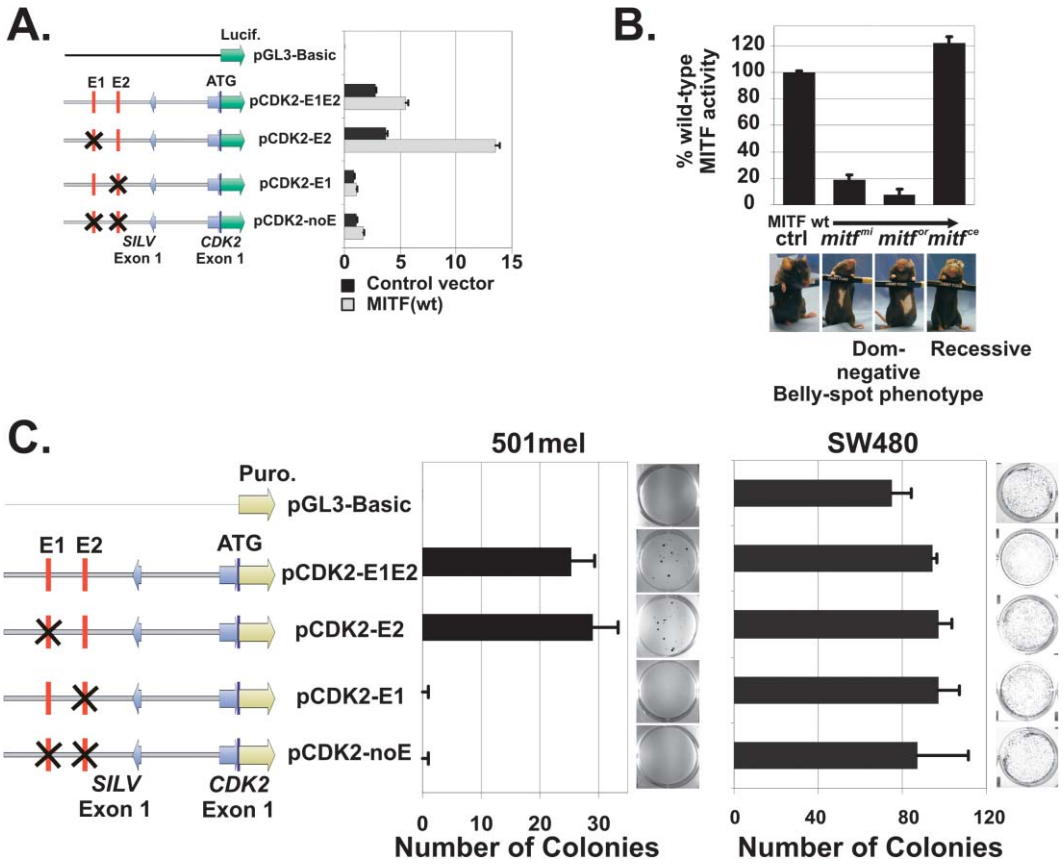

Figure 3. MITF modulates *CDK2* transcription via an E box (E2) within the enhancer element

A: Reporter assays of CDK2 point mutants. CDK2 reporters with point mutations were transfected into 501mel melanoma. Firefly luciferase activities in samples were normalized to Renilla luciferase activities in the same specimens. Ratios between firefly and Renilla luciferase (transfection efficiency control) activities are shown.

B: Dominant-negative but not null MITF mutants disrupt transactivation of CDK2 reporter (pCDK2-E1E2) by the wild-type protein. The wild-type CDK2 reporter was transfected into 501mel cells in the presence of wild-type MITF plus vector control or Mitf mutant (*Mitf*$^{Mi\text{-}or}$, *Mitf*$^{Mi\text{-}mi}$, or *Mitf*$^{mi\text{-}ce}$). The transfections were performed in triplicate, and standard errors are indicated with bars. The data are shown as percent wild-type MITF activity on the human CDK2 reporter after subtracting vector-only control. The belly spot phenotypes of corresponding heterozygous *Mitf* mutant are presented underneath. Wild-type MITF activity was repressed by Mitf$^{Mi\text{-}or}$ and Mitf$^{Mi\text{-}mi}$ (with belly spots) but not Mitf$^{mi\text{-}ce}$ (no belly spot).

C: Colony formation assay of pCDK2-puro constructs. Vectors expressing puromycin resistance gene driven by the CDK2 promoter-enhancer were constructed and transfected into 501mel (melanoma) or SW480 (nonmelanoma) as described in the Experimental Procedures section. Number of colonies were counted 2 weeks postselection and are shown together with a representative example.

terious to melanoma cell growth, although complementary approaches are required to reach this conclusion (see below), since the CDK2(dn) could theoretically carry out CDK2-independent inhibitory activities.

Correlation of CDK2 and MITF expression in human melanoma cell lines and primary human melanomas but not other cancers

As an independent means of examining the relevance of CDK2 regulation by MITF in vivo, mRNA levels of MITF and CDK2 were examined by quantitative RT-PCR in nine human melanoma cell lines and found to be tightly correlated (Figure 6A). In addition, microarray expression profiling data were examined from a series of primary human melanomas (Ramaswamy et al., 2001). To look for genes highly correlated with endogenous MITF expression in melanomas, we identified the genes best matching the MITF expression pattern using a Pearson correlation coefficient-based marker analysis algorithm. The significance of the correlation was computed as described in the Experimental Procedures section. Of the 16,063 genes analyzed, *CDK2* was significantly correlated to *MITF* in the ten primary melanomas ($p < 0.01$) (Figure 6B). Importantly, *CDK2* was not significantly correlated with *MITF* in nonmelanoma tumors (shown for lymphomas in Figure 6C). We also examined the protein levels of MITF and CDK2 in these nine melanoma cell lines and observed a correlation in protein expression. In contrast, the expression levels of three additional cyclin-dependent kinases (CDK1, CDK4, and CDK5) lacked correlation with MITF expression in these melanomas (Figure 6D). These observations provide independent support for the model that MITF resides in a transcriptional pathway with *CDK2* selectively within the melanocyte lineage.

MITF/CDK2 expression and sensitivity to roscovitine

The observed fluctuations in MITF and CDK2 mRNA and protein levels among the melanoma samples (Figure 7 and data not

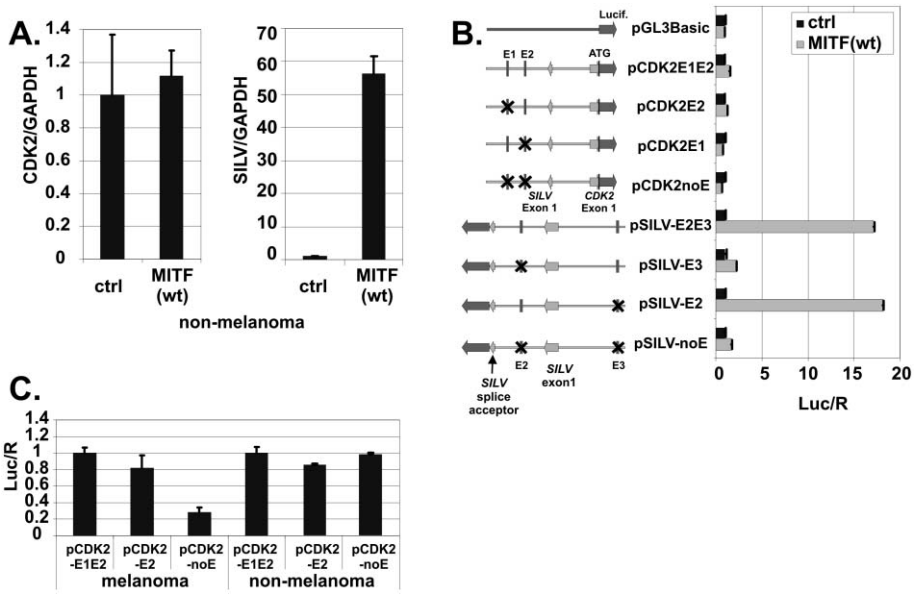

Figure 4. MITF does not regulate CDK2 transcription in nonmelanocytes

A: Endogenous CDK2 mRNA levels are not affected, while SILV mRNA levels are modulated by MITF overexpression in WI-38 fibroblasts. Total RNA was isolated 72 hr after infection. Quantitative RT-PCR was performed, and data were normalized to the expression level of the control gene. CDK2 and SILV mRNA levels in the control adenovirus-infected sample was normalized to 1.

B: In SW480 cells, MITF transactivates SILV but not CDK2 reporters in an E box-dependent fashion. Firefly luciferase activities in samples were normalized to Renilla luciferase activities in the same specimens. Relative luciferase activities are shown. The relative activities of control (vector)-stimulated reporters are normalized to 1.

C: Mutation of the E2 element lowers basal reporter activities in melanoma cells but has no effects in nonmelanocytes. CDK2 reporters were transfected into 501mel (melanoma) or SW480 cells (nonmelanoma), and luciferase activities were analyzed 48 hr after transfection. Firefly luciferase activities in samples were normalized to Renilla luciferase activities in the same specimens. The relative activities of pCDK2-E1E2 are normalized to 1 in both cell types.

shown) led us to ask whether expression level differences may be associated with altered sensitivity to CDK2 inhibitors and thereby predict treatment response for melanoma subsets. To test this hypothesis, melanoma cell lines were treated with dose titrations of the CDK2 inhibitor roscovitine (Rudolph et al., 1996), and LD50's were determined. Roscovitine inhibits CDK2/cyclinA and CDK2/cyclinE complexes by competing for the ATP binding domain in the kinase subunit. As shown in Figure 7, CDK2 expression correlated virtually perfectly with LD50 and indicated that lower CDK2 expression is associated with enhanced drug sensitivity, whereas high CDK2 expression confers relatively high resistance. In addition, we observed that SW480, a colon carcinoma cell line, appeared to be relatively resistant to roscovitine despite low CDK2 expression (Figure 7), consistent with previously published data that CDK2 is dispensable for the proliferation of these cells (Tetsu and McCormick, 2003). While numerous additional variables determine clinical responsiveness to antineoplastic agents, these data are consistent with the model that the unique regulation of CDK2 by MITF in melanomas is associated with a unique pattern of susceptibility to a new class of experimental therapeutics.

A critical role of CDK2 on melanoma growth and proliferation

Recent results show that CDK2 is not essential for the proliferation of colon carcinomas and cells from several other cancer types (Tetsu and McCormick, 2003). In addition, *Cdk2* knockout animals show no dramatic phenotypes other than sterility (Berthet et al., 2003; Ortega et al., 2003). However, ectopically expressed dominant-negative CDK2 produced a profound phenotype of G1-S arrest in several melanoma cell lines tested (data not shown), as well as suppression of clonogenic growth (Figure 5D). We therefore asked whether CDK2 might be of particular importance to melanoma growth. Toward this end, we designed a siRNA against CDK2 which could effectively knock down CDK2 protein expression as well as functionally reducing its kinase activity in transduced cells (Figure 8A). To investigate whether the CDK2 depletion affects cell proliferation and/or cell death, we then performed cell cycle analysis, short-term cell growth, and apoptosis assays upon introduction of retrovirus expressing siRNA against CDK2 in various melanoma lines (as compared to a control siRNA directed against the luciferase gene). FACS analysis showed CDK2 siRNA results in significant reduction of the S phase population in the five melanoma lines tested (Figure 8B). In addition, short-term growth was profoundly inhibited in these cells (Figure 8C and data not shown). On the other hand, we did not observe a large difference in cell death (data not shown), suggesting that CDK2 is primarily involved in melanoma proliferation, rather than survival. We also carried out colony growth assays in A375 melanoma cells. siRNA-mediated CDK2 depletion virtually abolished colony growth (Figure 8D). As a control, we performed the same experiment with the colon carcinoma cell line SW480. Consistent with the results obtained by Tetsu and McCormick (2003), we observed no significant difference in SW480 colony growth upon CDK2 downregulation (Figure 8D). These results are consistent with the possibility that melanoma cells behave differently than other cancers, such as colon carcinoma cells, in terms of a functional requirement for CDK2 activity for cell cycle progression.

Discussion

Here, we show that CDK2 is important for melanoma growth and proliferation. CDK2 has long been thought to be one of the key cell cycle regulators in the G1-S transition. However, its role has been challenged by three recent reports (Berthet et al., 2003; Ortega et al., 2003; Tetsu and McCormick, 2003). In colon cancer cell lines, CDK4 but not CDK2 inhibition is sufficient to cause cell cycle arrest following inhibition of the MAPK pathway (Tetsu and McCormick, 2003). Moreover, inhibition of CDK2

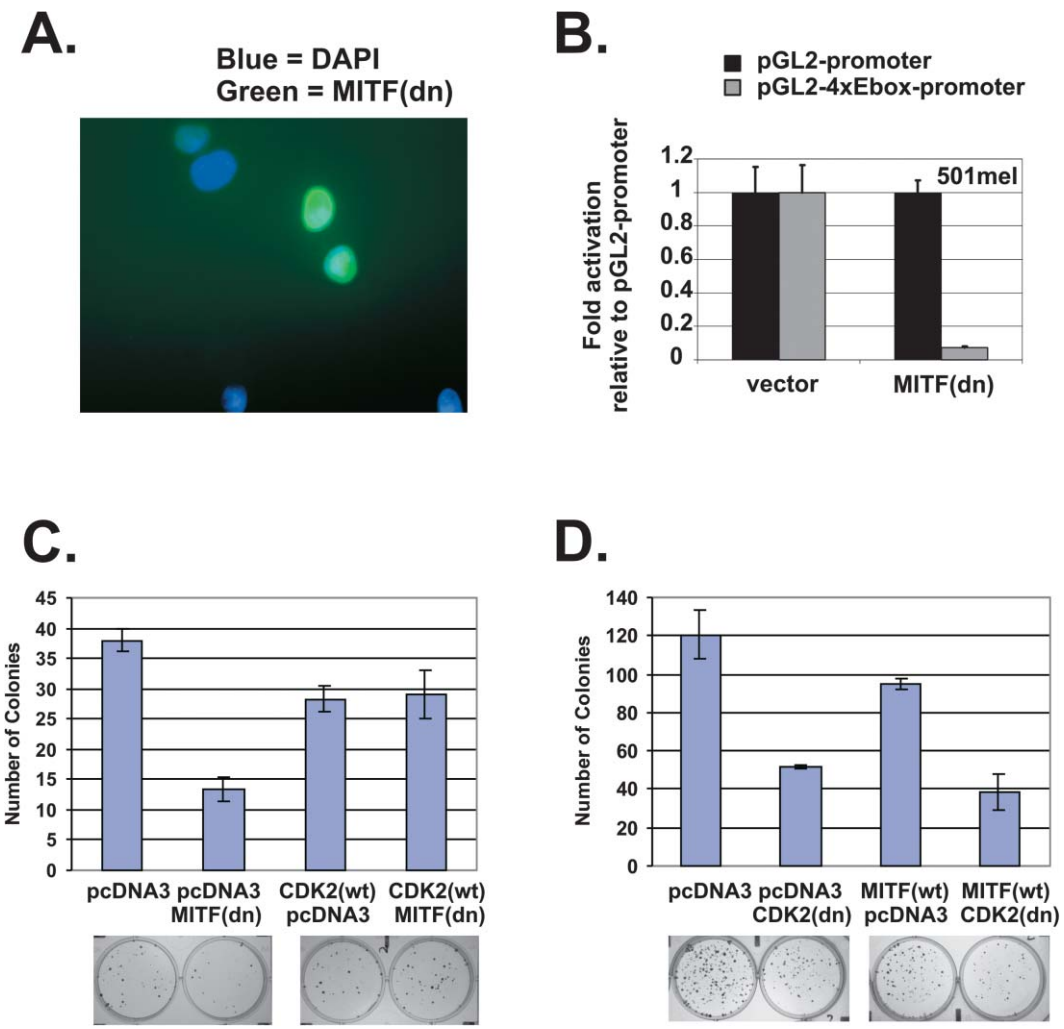

Figure 5. CDK2 resides downstream of MITF in melanoma colony growth assays

A: Immunofluorescence shows nuclear localization of DAPI (nuclei) and FITC (dominant-negative [dn] mutant of MITF) in 501mel melanoma cells.
B: Reporter assays of 4x E box in human 501mel melanoma cells show repression of basal transcription by dnMITF.
C: Rescue of MITF(dn) colony suppression by CDK2(wt). All experiments were done in triplicate. MITF(dn) expression vector was cotransfected with either control pcDNA3.1 or CDK2(wt) expression vector into 501mel cells. Puromycin was added to cultured media 48 hr posttransfection. Cells were stained with crystal violet once visible colonies appeared (>50 cells). Colonies were counted manually. Numbers of colonies are shown together with standard error.
D: Repression of colony formation by dominant-negative CDK2. CDK2(dn) expression vector was cotransfected with either control pcDNA3.1 or MITF(wt) expression vector into 501mel cells. Numbers of colonies are presented together with standard error.

with CDKN1B/p27KIP1, a dominant-negative CDK2, siRNA, or antisense against CDK2 did not prevent cell proliferation in these cells as well as several osteosarcomas and RB1-negative cervical cancer cell lines (Tetsu and McCormick, 2003). Our data also suggest that CDK2 is dispensable for colon carcinoma growth (Figure 8D). On the other hand, CDK2 appears to be of particular importance to human melanoma cells. Depletion of CDK2 with siRNA strongly suppressed colony growth of melanoma cells (Figure 8D). When CDK2 is partially depleted with retrovirus infection, both melanoma S phase population and growth rate are significantly reduced (Figures 8B and 8C). We also found that blocking CDK2 with a dominant-negative mutant suppressed colony-forming activity of melanoma cells (Figure 5D). In addition, overexpression of dominant-negative CDK2 arrested melanoma cells in G1-phase (data not shown). Together, these results suggest that CDK2 behaves as an important cell cycle regulator in melanoma cells. Inhibition of CDK2 thus warrants consideration as a therapeutic approach for melanomas, especially given the profound tolerance of the wild-type host to CDK2 suppression in the knockout setting.

Cdk2 null mice from Ortega et al. (2003) and Berthet et al. (2003) show no obvious coat color phenotype. This suggests that CDK2 is dispensable or that its function may be compensated for by other unknown factors during normal melanocyte development. Although human melanocytes that give rise to most cutaneous melanomas are thought to derive from epidermal compartment (differing from mice, in which melanocytes do not permanently reside in epidermis), the apparently normal hair follicle phenotype suggests that no major melanocytic defect is associated with CDK2 loss. It is therefore anticipated that siRNA against CDK2 would have little effect on cultured human primary melanocytes based on the in vivo data and the

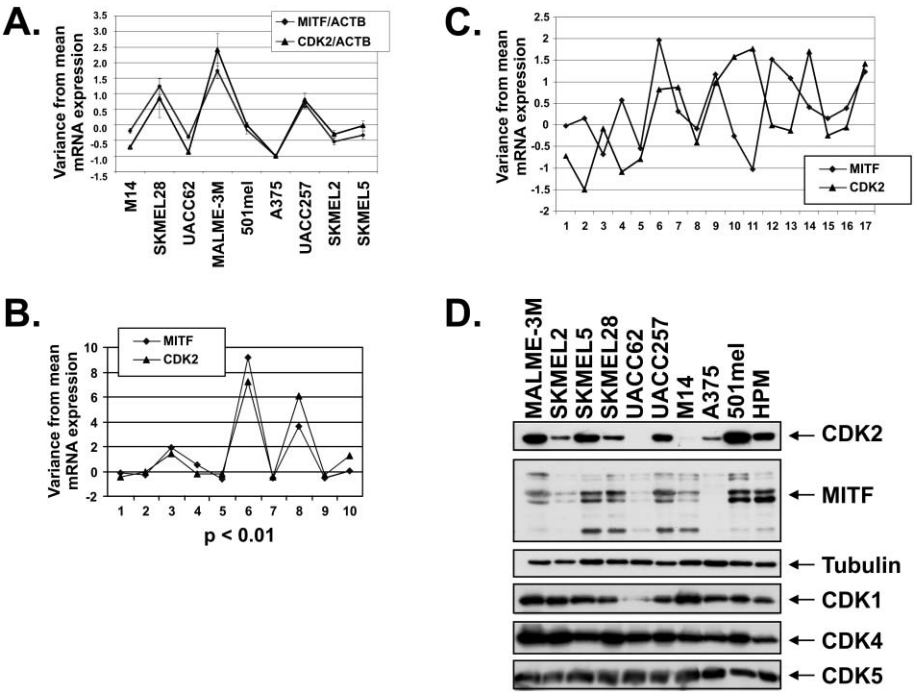

Figure 6. Correlations between MITF and CDK2 mRNA and protein levels in human melanomas

A: Correlations in human melanoma cell lines. Total RNA was extracted, and transcript levels of both genes were measured as described in the Experimental Procedures. Expression levels were normalized to that of ACTB (β-actin). The raw expression value for each gene was normalized to a mean of zero and standard deviation of one.

B: Correlations in human primary melanomas. Quantitative mRNA levels for both genes in ten primary melanomas were acquired from Affymetrix microarrays as described in the Experimental Procedures. The raw expression value for each gene was normalized to a mean of zero and standard deviation of one. Also see Experimental Procedures for p value calculation.

C: Lack of correlations in human lymphomas. Expression levels of CDK2 and MITF were acquired from Affymetrix microarrays. The raw expression value for each gene was normalized to a mean of zero and standard deviation of one.

D: Correlations at the protein level in human melanoma cell lines and lack of correlation for CDK1, CDK4, and CDK5.

fact that these cells are cycling very slowly and contain high levels of CDK2 and MITF.

CDK2 functions during the G1-S transition though RB1 phosphorylation and in S phase via regulation of DNA replication (Ekholm and Reed, 2000). Our results suggest that CDK2 is important for melanoma proliferation but do not distinguish between RB1-mediated G1 arrest versus blockage at other phases of the cell cycle. It will be interesting to see whether CDK2 depletion affects RB1 phosphorylation status in melanoma cells. Also, it will be interesting to study the effects of siCDK2 in a RB1 null setting in order to clarify the precise role of CDK2 in these cells.

One implication of the observations reported here is that CDK2 function is unique in melanoma, as compared to other tumor types examined by Tetsu and McCormick (2003), although it is formally possible that similar behavior may be discovered in other lineages. It is unclear at this stage how this comes about, or for that matter how other cell types survive without CDK2. Along these lines, we have examined the NCI-60 tumor cell line mRNA and protein expression databases (Staunton et al., 2001 and http://dtp.nci.nih.gov/mtargets/mt_index.html) for CDK2 levels and found that both mRNA and protein levels of CDK2 were particularly high in melanomas, as compared to all nonmelanoma cancers, in a statistically significant fashion ($p < 0.05$; data not shown). It is plausible that high CDK2 expression in melanomas is a consequence of turning on *SILV* transcription in these cells, since both genes share the same enhancer element. Alternatively, CDK2 might perform

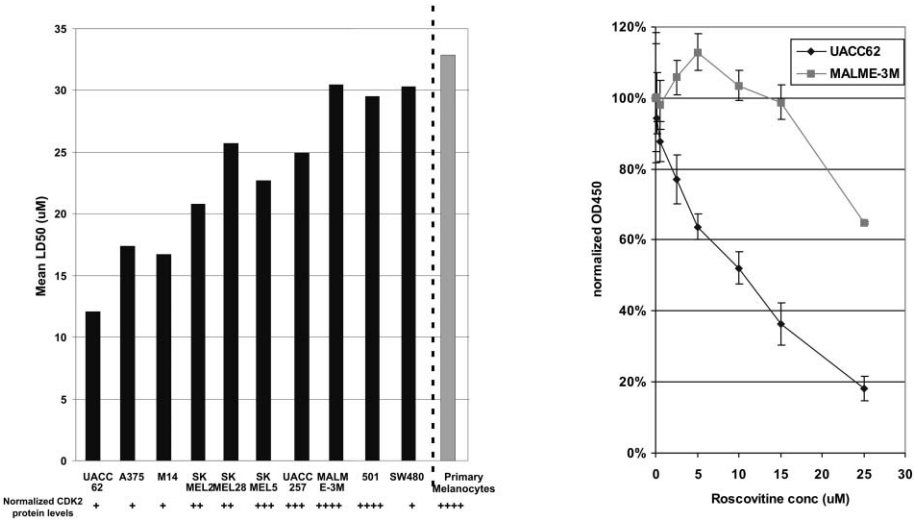

Figure 7. Sensitivities of melanoma cell lines to CDK2 inhibitor roscovitine correlate with endogenous CDK2 expression levels

Cell viability was measured at OD450 after WST-1 assay. LD50 for each cell line was obtained as described in the Experimental Procedures. The left panel presents the LD50 of various cell lines toward roscovitine. CDK2 expression levels in these cell lines are indicated at the bottom (lowest expression [+] to highest [++++]). The right panel presents representative response curves toward roscovitine in two melanoma cell lines.

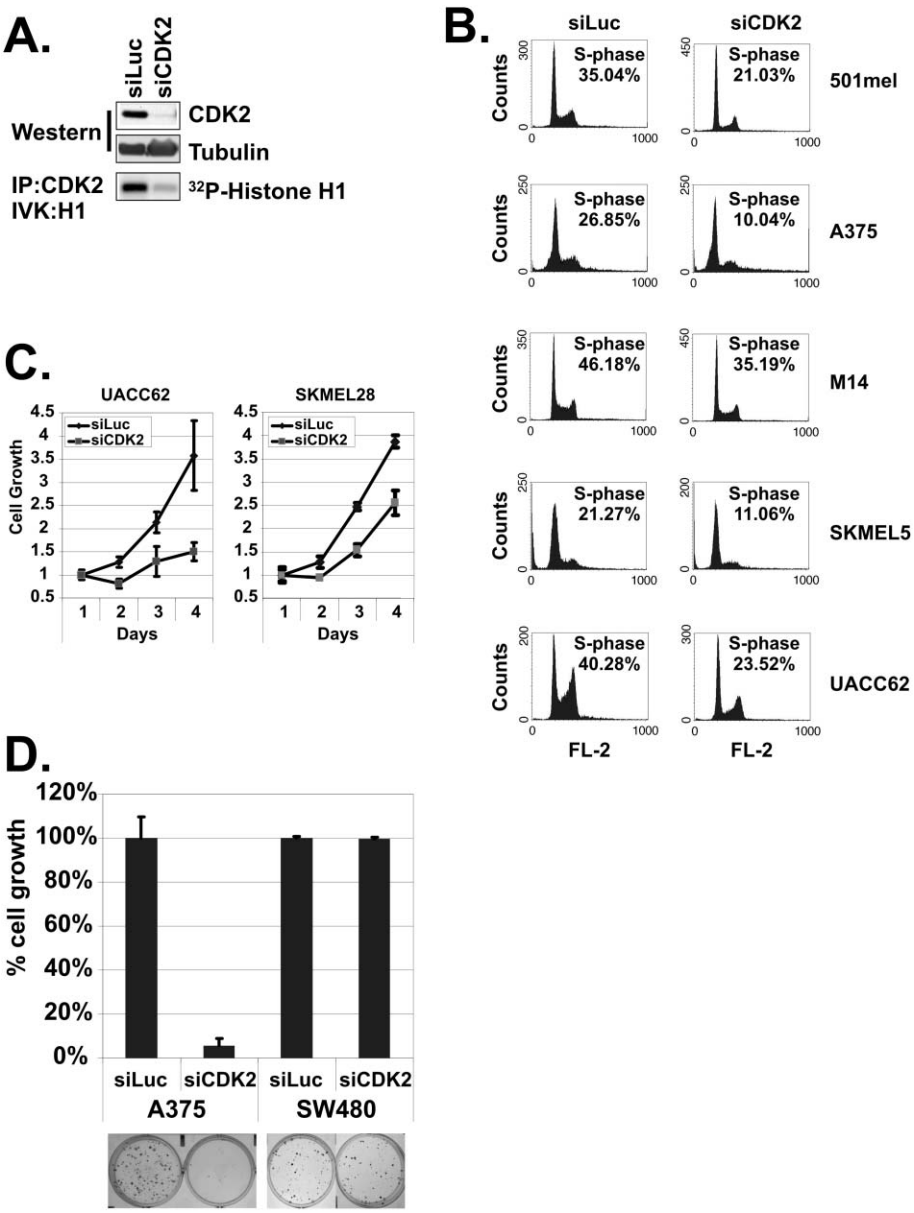

Figure 8. Effects of siRNA against CDK2 on melanoma growth and proliferation

A: siRNA against CDK2 downregulates CDK2 expression and kinase activity in melanoma cells. Western analysis and kinase assay were performed on melanoma lysates from cells infected with retrovirus expressing siRNA either against luciferase or against human CDK2.

B: Depletion of CDK2 decreases S phase population in melanoma cells.

C: Depletion of CDK2 slows down short-term proliferation of melanoma cells.

D: Downregulation of CDK2 dramatically reduced colony growth in melanoma (A375) but not colon carcinoma cells (SW480). Growth of cells transfected with control siLuc vectors is normalized to 100% for both lines.

different functional roles in melanomas, where higher levels of CDK2 may contribute to proliferation and/or growth.

MITF appears to modulate CDK2 expression in a melanocyte-specific manner, which is likely linked to its transcriptional regulation of *SILV/PMEL17/GP100*. It is important that CDK2 expression in nonmelanocytes appears to be independent of MITF (Figure 4A). In addition, reporter assays in nonmelanocytes indicated that the E box element to which MITF binds in melanocytes is irrelevant to basal CDK2 promoter activity and does not confer MITF responsiveness (Figures 4B and 4C). These observations suggest that CDK2 expression is regulated in a fundamentally distinct fashion in the melanocyte lineage, where it is potentially subject to fluctuations in MITF expressions. For example, melanocyte-stimulating hormone (MSH) and WNT signaling pathways are known to regulate MITF expression within melanocytes and may thus indirectly affect CDK2 expression as well (Englaro et al., 1995; McGill et al., 2002; Price et al., 1998).

It is noteworthy that, unlike many other melanocytic markers, MITF is expressed in nearly all human melanomas (Chang and Folpe, 2001), including nonpigmented ones. This observation suggests that MITF is critical to proliferation and/or survival. This possibility defines a role for MITF beyond regulation of melanocyte differentiation genes. One potential contributor to MITF's survival effect appears to be BCL2, which is transcriptionally regulated by MITF and whose knockout produces postnatal melanocyte loss (McGill et al., 2002; Veis et al., 1993). However, BCL2 is unlikely to fully account for MITF's viability function in melanoma cells, since BCL2 overexpression is incapable of rescuing melanoma clonogenic growth in the setting of MITF disruption (McGill et al., 2002). CDK2 is thus an attractive candidate to help explain the essential role of MITF in melanoma cells.

In this study, we found that downregulation of MITF represses colony formation by melanoma cells, suggesting that MITF may be required for melanoma growth/survival. This repression could be rescued by overexpression of wild-type CDK2, suggesting that CDK2 is one of MITF's downstream effectors essential to cellular proliferation. Together, the current work identifies CDK2 as a cell cycle-related target gene and also suggests that its modulation by MITF is functionally important to melanoma growth. Thus, the identification of CDK2 as a transcriptional target of MITF in melanocytes highlights a newly identified role for MITF in support of the cell cycle machinery. Moreover, our results suggest that CDK2 might be particularly important for melanoma proliferation. These observations not only help explain MITF's essential role in melanoma growth but also support CDK2 as a potential drug target for melanoma therapy. Moreover, the unique regulation of CDK2 transcription in melanoma, correlating between CDK2 (also MITF) expression and drug sensitivity, may help predict patients' responses to CDK2-targeted cancer treatment.

Experimental procedures

Cell culture and media

501mel was a gift from Dr. Ruth Halaban (Yale Medical School) and was maintained in Ham's F10 medium supplemented with 10% FBS. MeWo, SKMEL5, A375 melanomas, and WI-38 fibroblasts were purchased from ATCC. All other melanoma cell lines (M14, SKMEL28, UACC62, MALME-3M, UACC257, and SKMEL2) were obtained from NCI. SW480 colon carcinoma was a gift from Eric Fearon. SKMEL5, A375, and SW480 were cultured in DMEM with 10% FBS. All melanoma lines from NCI were maintained in RPMI with 10% FBS. MeWo was cultured in Ham's F10 with 10% FBS. WI-38 was cultured in MEM (Mod.) with 10% FBS. Human primary melanocytes were purchased from Clonetics or provided by Dr. Ruth Halaban and maintained in TICVA medium (F10 with penicillin/streptomycin/glutamine, 7.5% FBS, 50 ng/ml TPA, 225 μM IBMX, 1 μM Na_3VO_4, and 1 mM dbcAMP).

Microarray and gene correlation analyses

Expression profiling data on human primary tumors were collected using Affymetrix Hu6800 and Hu35KsubA high-density oligonucleotide microarrays as described elsewhere (Ramaswamy et al., 2001). Here, we specifically looked at primary melanomas and lymphomas. Expression values were given a lower threshold of 10 units and a ceiling of 16,000 units. For marker analyses, the data set was filtered to eliminate genes whose expression levels did not vary more than 5-fold or 50 absolute units across the data set. Of the 16,063 genes on the microarray, 11,187 and 13,177 genes passed this filter for the melanoma and lymphoma analyses, respectively. Marker analyses were performed using the Pearson correlation coefficient to identify genes with similar patterns of expression to MITF across the melanoma and lymphoma collections. Genes were sorted by their degree of correlation. To assess the significance of the correlation, we permutated the tumor sample labels 10,000 times and computed the Pearson correlation between MITF and CDK2 after each permutation. The distribution of permuted Pearson values indicated the number of times our permuted Pearson value exceeded our experimental Pearson value, which allowed us to assign a p value to our observation in both the melanoma and lymphoma datasets.

Construction of CDK2 reporters

A 2.8 kb fragment containing the first exon of CDK2 and flanking sequences was amplified from human genomic DNA (Roche) using primers 5′-GCA ATC CTA TGA CCA CGG CCT CCC AAA G-3′ and 5′-GTT TTC CAT GGA TTC CAC ACC ACC CTA TAC-3′. A smaller fragment was subsequently amplified from the 2.8 kb fragment with primers 5′-CGG GTA CCA TGC CTC GGC CTC CCA AGT AGT-3′ and 5′-GGC CAT GGA GCG CCA GCG AGT CGG GTC AGC-3′, digested with KpnI and NcoI, and inserted into pGL3-basic vector (Promega).

CDK2 reporter construct mutagenesis

Site-directed mutagenesis was performed using the QuickChange method (Stratagene) according to the supplier's recommendations. Mutagenesis primers were designed as follows: E1, 5′-CTGGGACTACAGGGAGGTGC CACCATGCC-3′ and 5′-GGCATGGTGGCACCTCCCTGTAGTCCCAG-3′; E2, 5′-CCCAGAGCCCTTTGAGGTGATGCTCAGCT-3′ and 5′-AGCTGAGC ATCACCTCAAAGGGCTCTGGG-3′.

Transfection and dual luciferase reporter assay

CDK2 and pGL2-4xE-box (Hemesath et al., 1994) reporter constructs were transfected using Fugene 6 (Roche) together with either pRC-CMV/MITF(wt) (encoding full-length M-form human MITF), pRC-CMV/MITF(mutant) (encoding murine M-form MITF lacking amino acid Arg218) (Hemesath et al., 1994; Motyckova et al., 2001; Wu et al., 2000) or pcDNA3.1 (Invitrogen) and pRL null (Promega). A total of 1 μg DNA was used for each transfection. Cell lysates were prepared 48 hr after transfection, the activities of firefly and Renilla luciferase were assayed using a Dual Luciferase kit (Promega) according to the manufacturer's recommendations, and signals were normalized for transfection efficiency to the internal Renilla controls.

pPL3-CDK2 constructs and colony formation assay

The pPL3-CDK2 vectors (with puromycin resistance) were constructed by replacing the luciferase coding sequence in corresponding luciferase reporters with puromycin CDS from pLPCX (Clontech). Colony growth assay was performed by transfecting 6 μg pCDK2-puro plasmid per well of 501mel in 6-well plates. Each transfection was done in triplicate. Puromycin was added to the media 24 hr posttransfection. Numbers of colonies were counted after fixation and crystal violet staining 14 days postselection.

ChIP

ChIP assays were performed with cells grown to logarithmic phase. Cells were harvested by scraping, homogenized in a hypotonic buffer (10 mM Tris-HCl [pH 7.4], 15 mM NaCl, 60 mM KCl, 1 mM EDTA, 0.1% Nonidet P40, 5% sucrose, 1× complete proteinase inhibitor cocktail [Roche]) on ice using a Dounce homogenizer. The nuclei were isolated by centrifugation onto a 10% sucrose pad and then crosslinked with 1% formaldehyde in PBS for 20 min at room temperature with gentle shaking. Nuclei were then spun down and resuspended in ChIPs buffer (10 mM Tris-HCl [pH 7.4], 100 mM NaCl, 60 mM KCl, 0.1% Nonidet P40, 1× complete proteinase inhibitor cocktail [Roche]) and sonicated by two 1 min pulses on ice using a Fisher dismembranator fitted with a microtip. Antibodies (rabbit anti-MITF, rabbit anti-BRN2 [sc-6029X; Santa Cruz], or rabbit anti-CDK2 [H-298; Santa Cruz]) were then added to a 10-fold ChIPs buffer diluted sample and incubated on a nutator for 3 hr at room temperature. Ultralink protein-A/G-beads (Pierce) were added to the sample and a control sample and incubated for an additional hour. Immunoprecipitates were then washed twice with ChIPs buffer, twice with 500 mM NaCl ChIPs buffer, and once with TE (pH 8). The immunoprecipitates were released from the beads by incubating at 65°C for 20 min in 1% SDS/TE and protein digested by proteinase K treatment side by side with an additional unprecipitated sample as input control. Crosslinks were released by heating at 70°C for 10 hr, and DNA was recovered by extraction with phenol and chloroform at high-salt (0.6 M Na Acetate [pH 8]) and then ethanol precipitated. Semiquantitative PCR was then performed on samples to amplify a fragment containing the second E box (E2) or the third E box (E3) in the human *CDK2/SILV* transcription initiation region. The forward and reverse primers for the E2 region are 5′-CAT AAG ATA CCC CAT TCT TTC TCC ACT T-3′ and 5′-GAG AAT GTG GTA TTG GGT AAG AAC AC-3′, respectively. The primers for the E3 region are 5′-CAT GGA GAA CTT CCA AAA GGT GG-3′ and 5′-TAC TCT CCC CAG GGA GTA TAA GT-3′.

Adenovirus infection and RNA preparation

Adenoviruses encoding wild-type MITF, dominant-negative mutant MITF, or vector control encoding a polypeptide were generated as previously described (Miller et al., 2004). Briefly, 10^6 cells were plated per 100 mm plate. On the second day, cells were overlaid with 2 ml serum-free F10 media containing 10 mM $MgCl_2$, and concentrated adenovirus was added at MOI 100. The cells were incubated at 37°C for half an hour, after which virus was removed and fresh full media was added. Total RNA was isolated with RNAqueous-4PCR kit (Ambion) at 48 or 72 hr after infection.

Real-time/quantitative PCR

The real-time PCR primers for human CDK2 were 5′-ATG GAG AAC TTC CAA AAG GTG GA and 5′-CAG GCG GAT TTT CTT AAG CG (IDT). The probes for human CDK2 were 5′-6-FAM-ATCGGAGAGGGCACGTACGGAGTTGT-TAMRA (PE Biosystems). The primers for human MITF were 5′-CGA GCT CAT GGA CTT TCC CTT A and 5′-CTT GAT GAT CCG ATT CAC CAA A (IDT). The probe was 5′-6-FAM-CCA TCC ACG GGT CTC TGC TCT CCA G (PE Biosystems). The primers for human β-actin (ACTB) were 5′-ATT GCC GAC AGG ATG CAG AA and 5′-GCT GAT CCA CAT CTG CTG GAA (IDT), and the probe was 5′-6-FAM-CAA GAT CAT TGC TCC TCC TGA GCG CA (IDT). The total volume of each reaction was 25 μl, including 12.5 μl 2× Master Mix without UNG (uracil-N-glycosylase), 0.625 μl MultiScribe Reverse Transcriptase and RNase inhibitor (PE Biosystems), 0.5 μl of each primer (10 μM stock), 0.25 μl of the probe (5 μM stock), and 1 μl of the template at 100 ng/μl. Reverse transcription proceeded at 48°C for 30 min. Then, 40 cycles of PCR reaction were carried out at 95°C for 15 s and at 60°C for 1 min. Real-time PCR was carried out using ABI PRISM 7700 Sequence Detection System (Applied Biosystems) with analysis using the integrated Sequence Detection System Software Version 1.7. Standard curves were generated for all primer sets to confirm linearity of signals over the experimentally measured ranges.

Western analysis

Cells were collected and lysed in 2× lysis/loading buffer (125 mM Tris [pH 6.8], 4.6% SDS, 20% glycerol, and 0.04% pyronin Y), resolved by electrophoresis in 12% SDS-polyacrylamide gels, and transferred to nitrocellulose membranes (Protran from Schleicher and Schuell). All proteins were detected using chemiluminescence and antibodies to CDK2 (Santa Cruz), MITF (C5), CDK1 (UpState), CDK4 (UpState), CDK5 (UpState), BCL2 (Santa Cruz), SILV (anti-PEP13h from Dr. Vincent Hearing), and α-tubulin (Sigma).

pcDNA3-5′trMi construct and colony formation assay

A DNA sequence encoding dominant-negative human MITF lacking the 5′ transactivation domain (used in colony assays; Figure 5) was cloned after PCR amplification into the BamH1/EcoRI sites of pcDNA3.1 (Invitrogen) construct carrying an engineered HA-tag 5′ of the basic region of MITF. 501mel cells were split into 6-well plates to give a confluency of 50% on the day of transfection. A total of 2.5 μg (for wt-MITF and dn-CDK2) or 5 μg (for dn-MITF and wt-CDK2) DNA including 10% pBabe-puro was transfected per well using Fugene6. For Figure 8, A375 and SW480 cells were cotransfected with 3 μg pSUPER-siLuc or pSUPER-siCDK2 and a puromycin-resistant gene expression vector. Puromycin (2 μg/ml) was added to media 48 hr posttransfection. Once visible colonies appeared (10–14 days), cells were fixed with 10% MeOH/10% HOAc for 20 min and stained with 0.4% crystal violet in 20% EtOH for 30 min. Plates were subsequently washed with water extensively and photographed. Colonies containing ≥50 cells were counted using the ChemiImager 5500 software. Alternatively, cells were then destained with 500 μl 10% methanol and 10% acetic acid in PBS for each well. The OD595-750 was used as measurement for cell numbers.

Immunofluorescence

Human 501mel cells were seeded onto poly-lysine-treated coverslips in 24-well plates and transfected the following day with 0.8 μg pcDNA3.1-HA/MITF(5′tr) using Lipofectamine 2000 (Gibco). Twenty-four hours after transfection, the cells were fixed with 3% formaldehyde and stained with FITC-conjugated rat high-affinity anti-HA monoclonal antibody (Roche) in 10% normal goat serum. Subsequently, the cells were washed twice with PBS, counterstained with DAPI, and photographed through a Nikon fluorescence microscope.

Cell proliferation assays and LD50 determination

WST-1 cell proliferation assays (Roche) were carried out 48 hr posttreatment of roscovitine (Calbiochem) to measure cell proliferation/viability. LD50 was calculated by fitting the linear range of these dose titratration curves (Figure 7 and data not shown).

CDK2 and MITF siRNA constructs, retrovirus infection, and cell growth assay

The pSUPER vector containing siRNA against CDK2 (NM_001798, nt 983–1001) or MITF (NM_000248, nt 738–756) was generated as described elsewhere (Brummelkamp et al., 2002). A fragment containing the H1 promoter and the hairpin was excised from pSUPER with EcoRI and XhoI and inserted into the p(si)^2-puro retrovirus vector. MEK293EBNA cells (2×10^6; Clontech) were transfected with VSVG, GAGPOL expression vectors, and p(si)^2-siCDK2 or p(si)^2-siMITF. Supernatant was harvested from day 2 to day 8 after transfection. Melanoma cells were infected with the 0.45 μm filtered supernatant in the presence of 8 μg/ml polybrene for 3 hr. The retrovirus supernatant was then removed, and fresh media were added to the cells. Forty-eight hours after infection, puromycin was added at a final concentration of 2 μg/ml to select for infected cells. Western analysis, CDK2 kinase assay, FACS analysis, and cell growth assay were performed starting at 48 hr after selection. For cell growth assay, retrovirus-infected cells were plated onto 6-well plates. Triplicate samples were plated for each sample at each time point. Cells were fixed from day 1 to day 4 after plating and stained with crystal violet. Cells were then destained with 500 μl 10% methanol and 10% acetic acid in PBS for each well. The OD595-750 was used as measurement for cell growth.

CDK2 kinase assay and cell cycle analysis

Cells were lysed with EBC buffer (50 mM Tris [pH 8.0], 100 mM NaCl, 0.5% NP-40) with phosphotase inhibitors (0.5 mM Na_3VO_4, 1 mM NaF, 10 mM β-glycerophosphate) and protease inhibitors (Roche) on ice for 30 min. Lysed cells were spun down, and protein concentration was measured with BCA Protein Assay Kit (Pierce) according to the manufacturer's instructions. Equal amount of total protein from each sample was incubated with agarose-conjugated anti-CDK2 antibody (Santa Cruz M2) for 120 min at 4°C. Immunocomplexes were washed with NETN buffer (20 mM Tris [pH 8.0], 100 mM NaCl, 1 mM EDTA, 0.5% NP-40) plus protease inhibitors and IPK buffer (50 mM Tris [pH 7.5], 10 mM $MgCl_2$, 1 mM DTT) with protease inhibitors. Histone H1 (2.5 μg), 20 μM cold ATP, and 1 μl of 10 mCi/ml γ-[^{32}P]-ATP were incubated with immunocomplexes in a 50 μl reaction at 30°C for 20 min. The samples were subjected to 12.5% SDS-PAGE. The gel was dried and subjected to autoradiography.

For cell cycle analysis, cells were pelleted and fixed in 70% EtOH for 30 min. Cells were washed with PBS once and stained with 1 mg/ml propidium iodide and 25 μg/ml RNase in PBS for 30 min. The cell cycle profiles were collected with FACSCaliber with Cellquest (Becton Dickinson) and analyzed with ModFit (Verity Software House) software.

Acknowledgments

We thank Dr. Ruth Halaban for useful discussions and for providing 501mel human melanoma and primary human melanocytes, Dr. Phil Hinds for CDK2 expression vectors, and Dr. Eric Fearon for SW480 colon carcinoma cells. In addition, Dr. Dov Shiffman is thanked for supplying reagents at an earlier stage of this project. We also thank Dr. Peter Sicinski, Dr. Mark Ewen, and Dr. Frank McCormick for advice and helpful comments on the manuscript. Dr. Jay P. Morgenstern is thanked for the VSVG and GAGPOL expression vectors. H.R.W. is a Swedish Wenner-Gren postdoctoral fellow, and S.R. is supported by a Harvard Medical School/NIH Training Grant in Molecular Hematology. This research was funded by a NIAMSD grant from the NIH (AR43369) to D.E.F., who is the Jan and Charles Nirenberg Fellow in Pediatric Oncology at Dana-Farber Cancer Institute.

Received: May 9, 2004
Revised: September 14, 2004
Accepted: October 6, 2004
Published: December 20, 2004

References

Adachi, N., and Lieber, M.R. (2002). Bidirectional gene organization: a common architectural feature of the human genome. Cell *109*, 807–809.

Adema, G.J., de Boer, A.J., van 't Hullenaar, R., Denijn, M., Ruiter, D.J., Vogel, A.M., and Figdor, C.G. (1993). Melanocyte lineage-specific antigens recognized by monoclonal antibodies NKI-beteb, HMB-50, and HMB-45 are encoded by a single cDNA. Am. J. Pathol. *143*, 1579–1585.

Altschul, S.F., Madden, T.L., Schaffer, A.A., Zhang, J., Zhang, Z., Miller, W., and Lipman, D.J. (1997). Gapped BLAST and PSI-BLAST: a new generation of protein database search programs. Nucleic Acids Res. *25*, 3389–3402.

Bentley, N.J., Eisen, T., and Goding, C.R. (1994). Melanocyte-specific expression of the human tyrosinase promoter: activation by the microphthalmia gene product and role of the initiator. Mol. Cell. Biol. *14*, 7996–8006.

Berthet, C., Aleem, E., Coppola, V., Tessarollo, L., and Kaldis, P. (2003). Cdk2 knockout mice are viable. Curr. Biol. *13*, 1775–1785.

Brummelkamp, T.R., Bernards, R., and Agami, R. (2002). A system for stable expression of short interfering RNAs in mammalian cells. Science *296*, 550–553.

Chang, K.L., and Folpe, A.L. (2001). Diagnostic utility of microphthalmia transcription factor in malignant melanoma and other tumors. Adv. Anat. Pathol. *8*, 273–275.

Du, J., Miller, A.J., Widlund, H.R., Horstmann, M.A., Ramaswamy, S., and Fisher, D.E. (2003). MLANA/MART1 and SILV/PMEL17/GP100 are transcriptionally regulated by MITF in melanocytes and melanoma. Am. J. Pathol. *163*, 333–343.

Ekholm, S.V., and Reed, S.I. (2000). Regulation of G(1) cyclin-dependent kinases in the mammalian cell cycle. Curr. Opin. Cell Biol. *12*, 676–684.

Englaro, W., Rezzonico, R., Durand-Clement, M., Lallemand, D., Ortonne, J.P., and Ballotti, R. (1995). Mitogen-activated protein kinase pathway and AP-1 are activated during cAMP-induced melanogenesis in B-16 melanoma cells. J. Biol. Chem. *270*, 24315–24320.

Hemesath, T.J., Steingrimsson, E., McGill, G., Hansen, M.J., Vaught, J., Hodgkinson, C.A., Arnheiter, H., Copeland, N.G., Jenkins, N.A., and Fisher, D.E. (1994). microphthalmia, a critical factor in melanocyte development, defines a discrete transcription factor family. Genes Dev. *8*, 2770–2780.

Hodgkinson, C.A., Moore, K.J., Nakayama, A., Steingrimsson, E., Copeland, N.G., Jenkins, N.A., and Arnheiter, H. (1993). Mutations at the mouse microphthalmia locus are associated with defects in a gene encoding a novel basic-helix-loop-helix-zipper protein. Cell *74*, 395–404.

McGill, G.G., Horstmann, M., Widlund, H.R., Du, J., Motyckova, G., Nishimura, E.K., Lin, Y.L., Ramaswamy, S., Avery, W., Ding, H.F., et al. (2002). Bcl2 regulation by the melanocyte master regulator Mitf modulates lineage survival and melanoma cell viability. Cell *109*, 707–718.

Miller, A.J., Du, J., Rowan, S., Hershey, C.L., Widlund, H.R., and Fisher, D.E. (2004). Transcriptional regulation of the melanoma prognostic marker melastatin (TRPM1) by MITF in melanocytes and melanoma. Cancer Res. *64*, 509–516.

Motyckova, G., Weilbaecher, K.N., Horstmann, M., Rieman, D.J., Fisher, D.Z., and Fisher, D.E. (2001). Linking osteopetrosis and pycnodysostosis: regulation of cathepsin K expression by the microphthalmia transcription factor family. Proc. Natl. Acad. Sci. USA *98*, 5798–5803.

Ortega, S., Prieto, I., Odajima, J., Martin, A., Dubus, P., Sotillo, R., Barbero, J.L., Malumbres, M., and Barbacid, M. (2003). Cyclin-dependent kinase 2 is essential for meiosis but not for mitotic cell division in mice. Nat. Genet. *35*, 25–31.

Price, E.R., Horstmann, M.A., Wells, A.G., Weilbaecher, K.N., Takemoto, C.M., Landis, M.W., and Fisher, D.E. (1998). α-Melanocyte-stimulating hormone signaling regulates expression of microphthalmia, a gene deficient in Waardenburg syndrome. J. Biol. Chem. *273*, 33042–33047.

Ramaswamy, S., Tamayo, P., Rifkin, R., Mukherjee, S., Yeang, C.H., Angelo, M., Ladd, C., Reich, M., Latulippe, E., Mesirov, J.P., et al. (2001). Multiclass cancer diagnosis using tumor gene expression signatures. Proc. Natl. Acad. Sci. USA *98*, 15149–15154.

Rudolph, B., Saffrich, R., Zwicker, J., Henglein, B., Muller, R., Ansorge, W., and Eilers, M. (1996). Activation of cyclin-dependent kinases by Myc mediates induction of cyclin A, but not apoptosis. EMBO J. *15*, 3065–3076.

Shiffman, D., Brooks, E.E., Brooks, A.R., Chan, C.S., and Milner, P.G. (1996). Characterization of the human cyclin-dependent kinase 2 gene. Promoter analysis and gene structure. J. Biol. Chem. *271*, 12199–12204.

Silvers, W.K. (1979). The Coat Colors of Mice: A Model for Mammalian Gene Action and Interaction (New York: Springer-Verlag).

Staunton, J.E., Slonim, D.K., Coller, H.A., Tamayo, P., Angelo, M.J., Park, J., Scherf, U., Lee, J.K., Reinhold, W.O., Weinstein, J.N., et al. (2001). Chemosensitivity prediction by transcriptional profiling. Proc. Natl. Acad. Sci. USA *98*, 10787–10792.

Tachibana, M., Perez-Jurado, L.A., Nakayama, A., Hodgkinson, C.A., Li, X., Schneider, M., Miki, T., Fex, J., Francke, U., and Arnheiter, H. (1994). Cloning of MITF, the human homolog of the mouse microphthalmia gene and assignment to chromosome 3p14.1-p12.3. Hum. Mol. Genet. *3*, 553–557.

Tassabehji, M., Newton, V.E., and Read, A.P. (1994). Waardenburg syndrome type 2 caused by mutations in the human microphthalmia (MITF) gene. Nat. Genet. *8*, 251–255.

Tetsu, O., and McCormick, F. (2003). Proliferation of cancer cells despite CDK2 inhibition. Cancer Cell *3*, 233–245.

Veis, D.J., Sorenson, C.M., Shutter, J.R., and Korsmeyer, S.J. (1993). Bcl-2-deficient mice demonstrate fulminant lymphoid apoptosis, polycystic kidneys, and hypopigmented hair. Cell *75*, 229–240.

Wagner, S.N., Wagner, C., Hofler, H., Atkinson, M.J., and Goos, M. (1995). Expression cloning of the cDNA encoding a melanoma-associated Ag recognized by mAb HMB-45. Identification as melanocyte-specific Pmel 17 cDNA. Lab. Invest. *73*, 229–235.

Widlund, H.R., Horstmann, M.A., Price, E.R., Cui, J., Lessnick, S.L., Wu, M., He, X., and Fisher, D.E. (2002). β-catenin-induced melanoma growth requires the downstream target Microphthalmia-associated transcription factor. J. Cell Biol. *158*, 1079–1087.

Wu, M., Hemesath, T.J., Takemoto, C.M., Horstmann, M.A., Wells, A.G., Price, E.R., Fisher, D.Z., and Fisher, D.E. (2000). c-Kit triggers dual phosphorylations, which couple activation and degradation of the essential melanocyte factor Mi. Genes Dev. *14*, 301–312.

Yasumoto, K., Yokoyama, K., Shibata, K., Tomita, Y., and Shibahara, S. (1994). Microphthalmia-associated transcription factor as a regulator for melanocyte-specific transcription of the human tyrosinase gene. Mol. Cell. Biol. *14*, 8058–8070.

Yasumoto, K., Mahalingam, H., Suzuki, H., Yoshizawa, M., and Yokoyama, K. (1995). Transcriptional activation of the melanocyte-specific genes by the human homolog of the mouse Microphthalmia protein. J. Biochem. (Tokyo) *118*, 874–881.

Yasumoto, K., Yokoyama, K., Takahashi, K., Tomita, Y., and Shibahara, S. (1997). Functional analysis of microphthalmia-associated transcription factor in pigment cell-specific transcription of the human tyrosinase family genes. J. Biol. Chem. *272*, 503–509.